Supplementary Information

Efficient Green Electroluminescence Enabled by a Cyano-Modified Double-Boron-Embedded Multi-Resonance Framework

Zeyuan Ye,[a,b]† Chenghao Gui,[a]† Xiaoyu Guo,[a] Shengbing Xiao,[a] Zhuixing Xue,[a] Dongyu Xu,[a] Jingsheng Miao,[a] Shaolong Gong,[b] Xiaosong Cao[a]* and Chuluo Yang[a]

[a] Z. Ye, C. Gui, X. Guo, Dr. S. Xiao, Z. Xue, D. Xu, Dr. J. Miao, Dr. X. Cao, Prof. C. Yang
Shenzhen Key Laboratory of New Information Display and Storage Materials, College of Materials Science and Engineering, Shenzhen University, Shenzhen, 518060 (P. R. China)
E-mail: xcao@szu.edu.cn

[b] Z. Ye, Prof. S. Gong
College of Chemistry and Molecular Sciences, Hubei Key Lab on Organic and Polymeric Optoelectronic Materials, Wuhan University, Wuhan, 430072 (P. R. China)

† These authors contributed equally to this work.

Table of Contents

1. Experimental Section

1.1. Materials and Methods

All raw materials and anhydrous solvents were commercially available and used without further purification. The reactions were carried out under the protection of the high-purity argon atmosphere. All reactions were heated by metal sand bath (WATTCAS, LAB-500, https://www.wattcas.com). NMR measurements were conducted on Bruker Advance 400 (or 500) spectrometer. Tetramethylsilane was used as the internal standard and $CDCl_3$ as the solvent. The high-resolution mass spectrometry (HR-MS) for the compounds was conducted on a Thermo Scientific LTQ Orbitrap XL with ESI ion source.

1.2. Synthesis

The synthesis of **DBPXZ-Cl** is referenced from published article.[1]

Synthesis of DBPXZ: The intermediate **DBPXZ-Cl** (1.00 g, 1.06 mmol), $Pd_2(dba)_3$ (0.05 g, 0.05 mmol), S-Phos (0.07 g, 0.16 mmol) and *t*-BuOK (0.04 g, 3.18 mmol) were dissolved in Toluene/EtOH (10 mL/1 mL) under argon atmosphere, then the reaction was stirred at 100 ºC for 1 h. After cooling to room temperature, the product was extracted with dichloromethane and water, and the combined organic layer was dried over anhydrous Na_2SO_4, solvent was removed by rotary evaporation. Subsequently, the resultant crude product underwent purification through the employment of silica gel column chromatography (eluent: petroleum ether/dichloromethane = 7:1, *v/v*), giving the **DBPXZ** as a yellow solid (0.42 g, yield 45%). **DBPXZ:** ^{1}H NMR (500 MHz, $CDCl_3$) δ (ppm): 10.22 and 10.17 (s and s, 1H), 8.64 and 8.28 (d and d, J = 7.2 Hz, 2H), 7.85 (s, 2H), 7.62 (d, J = 8.2 Hz, 2H), 7.55–7.34 (m, 2H), 7.32 – 7.26 (m, 3H), 7.16 (d, J = 8.3 Hz, 4H), 7.07 (t, J = 7.6 Hz, 2H), 6.99 (s, 2H), 6.94 (s, 2H), 6.47 (s, 2H), 5.88 (s, 1H), 2.46 (s, 6H), 1.79 (s, 12H). ^{13}C NMR (126 MHz, $CDCl_3$) δ (ppm): 149.2, 147.5, 145.4, 142.7, 138.9, 136.6, 135.9, 130.3, 130.0, 129.0, 126.1, 124.2, 123.7, 119.5, 118.4, 117.9, 117.4, 114.9, 110.2, 108.7, 21.3, 17.1, 17.0. HRMS (ESI) *m/z* of $C_{60}H_{44}B_2N_4O_2$ for $[M+H]^+$: calcd 876.2296; found 876.2310.

Synthesis of DBPXZ-CN: The intermediate **DBPXZ-Cl** (2.00 g, 2.12 mmol), (4-cyanophenyl)boronic acid (0.94 g, 6.36 mmol), $Pd(PPh_3)_4$ (0.24 g, 0.21 mmol) and K_2CO_3 (1.17 g, 8.48 mmol) were added to a degassed solvent mixture of Toluene/EtOH/H_2O (40 mL/20 mL/20 mL) an argon atmosphere. After blowing argon for 15 minutes, the reaction was stirred at 90 ºC for 12 h. After cooling to room temperature, the mixture was extracted with dichloromethane, and the organic layer was collected. The solvent was subsequently removed by rotary evaporation. Subsequently, the resultant crude product underwent purification through the employment of silica gel column chromatography (eluent: petroleum ether/dichloromethane = 5:1, *v/v*), giving the **DBPXZ-CN** as a yellow solid (1.32 g, yield 58%). **DBPXZ-CN:** ^{1}H NMR (400 MHz, $CDCl_3$): δ (ppm)

10.23 and 10.21 (s and s, 1H), 8.67 and 8.36 (d and d, J = 7.1 Hz, 2H), 7.81 (s, 2H), 7.72–7.77 (m, 2H), 7.65 (d, J = 8.4 Hz, 4H), 7.51 (d, J = 8.5 Hz, 4H), 7.44 (t, J = 7.6 Hz, 1H), 7.22 (t, J = 7.9 Hz, 3H), 7.17 (d, J = 8.0 Hz, 2H), 7.11 (t, J = 7.4 Hz, 2H), 7.03 (t, J = 7.6 Hz, 2H), 6.98 (s, 2H), 6.93 (s, 2H), 6.40 (s, 2H), 5.86 (s, 1H), 2.45 (s, 6H), 1.86 (s, 12H). ^{13}C NMR (126 MHz, $CDCl_3$) δ (ppm): 149.5, 149.3, 147.6, 146.2, 145.8, 143.1, 142.9, 138.3, 137.1, 136.7, 136.2, 135.6, 132.5, 131.6, 130.1, 129.7, 129.1, 128.2, 125.4, 123.6, 123.4, 119.6, 118.8, 118.4, 117.8, 116.9, 111.3, 106.4, 104.7, 21.4, 17.3, 17.1. HRMS (ESI) *m/z* of $C_{74}H_{50}B_2N_6O_2$ for $[M+H]^+$: calcd 1076.4176; found 1076.4203.

1.3. Single Crystal X-ray Crystallography

The single crystal of the target compound **DBPXZ-CN** was prepared from a methanol/chlorobenzene solution by slow evaporation. X-ray single-crystal data were collected on a Bruker D8 Venture diffractometer using CuKα radiation (λ = 1.54178 Å) as the source. The selected crystal was kept at 170.0 K during data collection. Using Olex2[2], the structure was solved with the ShelXT[3] structure solution program using intrinsic phasing and refined with the ShelXL[4] refinement package using least-squares minimization. Selected crystal data are listed in **Table S6**. All crystallographic information in CIF format has been deposited at the Cambridge Crystallographic Data Centre (CCDC) under deposition number 2528545 for DBPXZ-CN via the CCDC website.

1.4. Quantum Chemical Calculations

All quantum chemical calculations were performed using the Gaussian 16 software package. Geometry optimizations and electronic structure calculations were carried out by density functional theory (DFT) at the b3lyp/6-31g(d,p) level. Grimme's D3 dispersion correction with Becke–Johnson damping was applied to account for long-range dispersion interactions. Time-dependent DFT (TD-DFT) calculations were also performed at the same level of theory.

To explore the conformational interconversion dynamics, we employed transition-state (TS) searches at the same level of theory. Initially, a relaxed potential energy surface (PES) scan was performed to locate the highest-energy point along the reaction pathway connecting the conformers. This geometry was then used as the starting point for a full TS optimization using the opt=(ts,calcfc) option. The optimized TS structures were confirmed by the presence of a single imaginary frequency corresponding to the interconversion mode, thereby validating the nature of the transition state and the calculated barrier for the conformational change.

The vertical transition energies of the S_1, T_1, and T_2 states, as well as the corresponding spin–orbit

coupling (SOC) matrix elements at the optimized S_1 geometry, were evaluated at the b3lyp/6-31g(d,p) levels. The SOC matrix elements between the singlet (S_1) and triplet (T_n, n = 1–3) states were calculated using the PySOC program, assuming that the three triplet sublevels (m = 0, ±1) are degenerate, i.e.,

$$\langle S_1|\hat{H}_{soc}|T_1\rangle = \sqrt{\sum_{m=0,\pm1}\langle S_1|\hat{H}_{so}|T_1{}^m\rangle^2},$$

where $\hat{H}_{soc}$ denotes the spin–orbit coupling Hamiltonian.[5]

1.5. Thermal and Electrochemical Characterization

Thermogravimetric analysis (TGA) was undertaken using TGA-Q50 Instrument (TA Instruments, America) at a heating rate of 10 °C/min from 50 °C to 800 °C under nitrogen flushing. The thermal decomposition temperatures (T_d) were determined by the recorded temperature at 5% weight loss. Cyclic voltammetry (CV) measurements were carried out on a CHI600 electrochemical analyzer (Chenhua, China) at room temperature and a scan speed of 50 mV s^{-1}, with a conventional three-electrode system consisting of a glassy carbon working electrode, a platinum wire auxiliary electrode, and an Ag/AgCl standard electrode using as the reference electrode. The supporting electrolyte was 0.1 M tetrabutylammonium hexafluorophosphate (Bu_4NPF_6) in anhydrous dichloromethane solution, and ferrocene was added as a calibrant in the whole measurement. The HOMO energy levels of the compounds were calculated according to the formula: E_{HOMO} (eV) = - [4.8 + ($E_{1/2(ox/red)}$ - $E_{1/2(Fc+/Fc)}$)] eV. The LUMO energy levels of the compounds were then deduced from the HOMO levels and the UV-Vis absorption onsets of the longer wavelength.

1.6. Photophysical Characterization

The UV-vis absorption spectra were obtained on a Shimadzu UV-2600 spectrophotometer (Shimadzu, Japan) at room temperature with a concentration of 1×10^{-5} M. Phosphorescence spectra were measured on a Hitachi F-7100 fluorescence spectrophotometer at 77 K. The transient photoluminescence (PL) decay curves were obtained by FluoTime 300 (PicoQuant GmbH) with a Picosecond Pulsed UV-LASTER (LASTER375) as the excitation source. The solid-state PL quantum efficiencies (Φ_{PLS}) were measured on a Hamamatsu UV-NIR absolute PL quantum yield spectrometer (C13534, Hamamatsu Photonics) equipped with an integrating sphere. The integrating sphere was purged with dry argon to maintain an inert atmosphere and all the samples were excited at 320 nm. Nanosecond time-resolved transient absorption spectra and decay kinetics were measured on LFP instrument (LP 980, Edinburgh Instruments LTD). The pump laser beam and the probe beam crossed perpendicularly through the liquid sample in a quartz cuvette (10 mm × 10 mm). A dynamic decay curve was recorded with a digital phosphor oscilloscope (TDS 3012C, Tektronix Inc.).

1.7. Analysis of Rate Constants

The estimation of rate constants pertaining to radiative decay (k_r) and nonradiative decay (k_{nr}) transitioning from S_1 to S_0, as well as the rate constants associated with intersystem crossing (k_{ISC}) and reverse intersystem crossing (k_{RISC}), can be accomplished by employing the subsequent equations.[6-8]

$$k_r = \Phi_p k_p + \Phi_d k_d \approx \Phi_p k_p \quad \text{Eq.(1)}$$

$$k_{nr} = \frac{1-\Phi_{PL}}{\Phi_{PL}} k_r \quad \text{Eq.(2)}$$

$$k_{ISC} = k_p - k_r - k_{nr} \quad \text{Eq.(3)}$$

$$k_{RISC} = \left(k_p k_d \Phi_d\right)/\left(k_{ISC}\Phi_p\right) \quad \text{Eq.(4)}$$

Where k_p and k_d represent the decay rate constants for prompt and delayed fluorescence, respectively, which are in reciprocal relationship with the decay time constants (τ_p and τ_d) experimentally determined from transient PL characteristics. Φ_p and Φ_d indicate prompt and delayed fluorescence components and can be distinguished from the total Φ_{PL} by comparing the integrated intensities of prompt (r_p) and delayed components (r_d) in the transient PL spectra. r_p and r_d were determined using τ_p and τ_d and fitting parameter (A_p, A_d) as follows.

$$I(t) = A_p e^{-\frac{1}{\tau_p}} + A_d e^{-\frac{1}{\tau_d}} \quad \text{Eq.(5)}$$

$$r_p = A_p\tau_p/(A_p\tau_p + A_d\tau_d) \quad \text{Eq.(6)}$$

$$r_d = A_d\tau_d/(A_p\tau_p + A_d\tau_d) \quad \text{Eq.(7)}$$

1.8. Device Fabrication and Measurement

The ITO coated glass substrates with a sheet resistance of 15 Ω square^{-1} were consecutively ultrasonicated with acetone/ethanol and dried with nitrogen gas flow, followed by 20 min ultraviolet light-ozone (UVO) treatment in a UV-ozone surface processor (PL16 series, Sen Lights Corporation). Then the sample was transferred to the deposition system. Both 8-hydroxyquinolinolato-lithium (Liq) as electron injection layer and aluminum (Al) as cathode layer were deposited by thermal evaporation at 5×10^{-5} Pa. The organic layers were deposited at the rates of 0.2-3 Å/s. After the organic film deposition, Liq and Al layer were deposited with rates of 0.1 and 3 Å/s, respectively. The emitting area of the device is about 0.09 cm^2. The current density-voltage-luminance (*J-V-L*), EQE-*L* curves and electroluminescence spectra were measured using a Keithley 2400 source meter and an absolute EQE measurement system (C9920-12, Hamamatsu Photonics, Japan).

2. Schemes, Figures and Tables

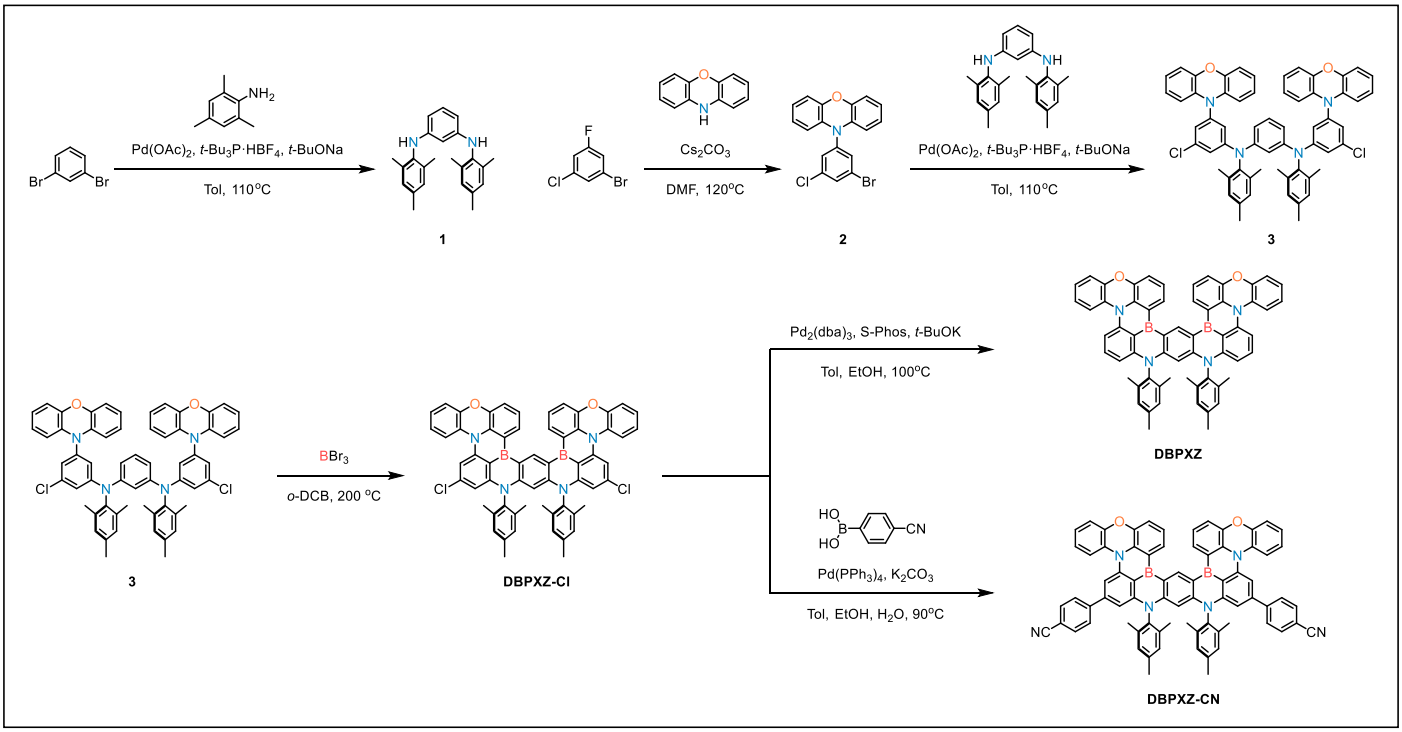

Scheme S1. Synthetic route of **DBPXZ** and **DBPXZ-CN**.

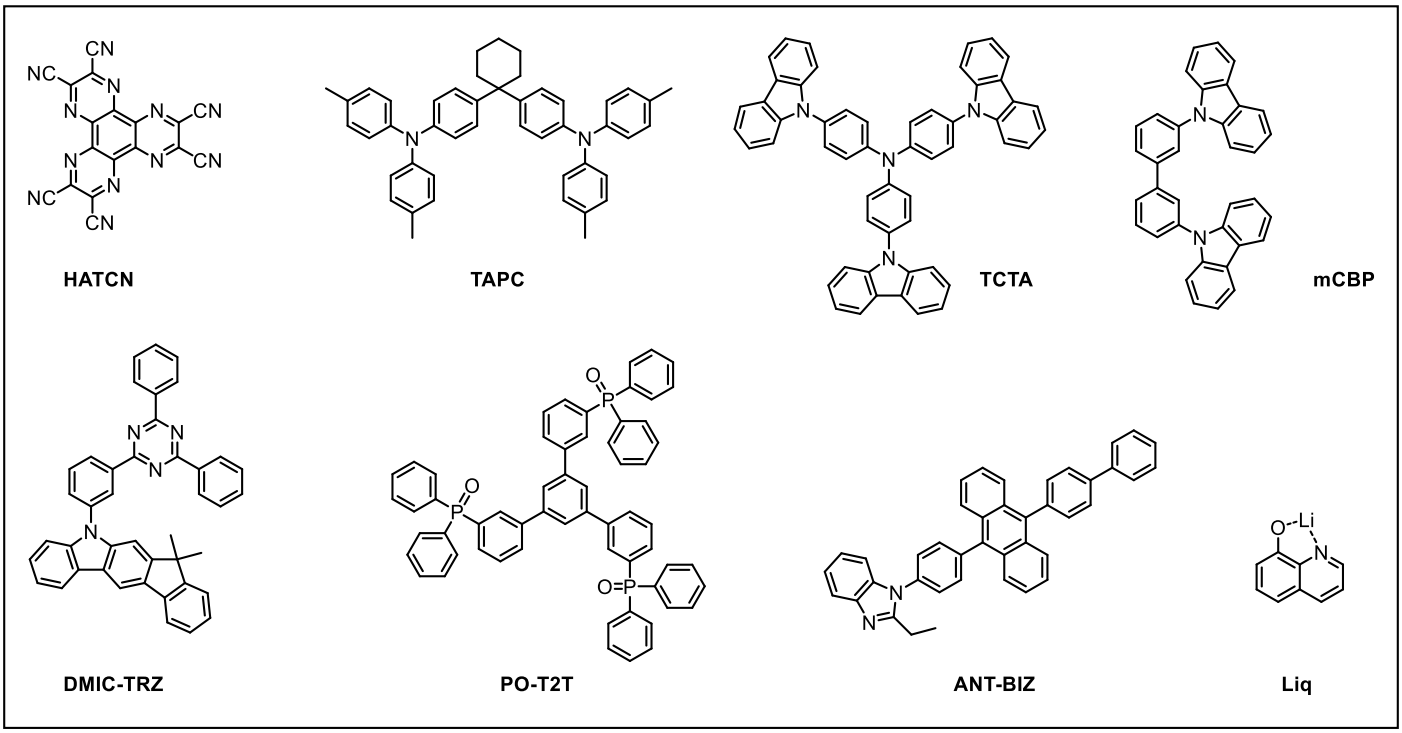

Scheme S2. Chemical structures of materials utilized for device fabrication.

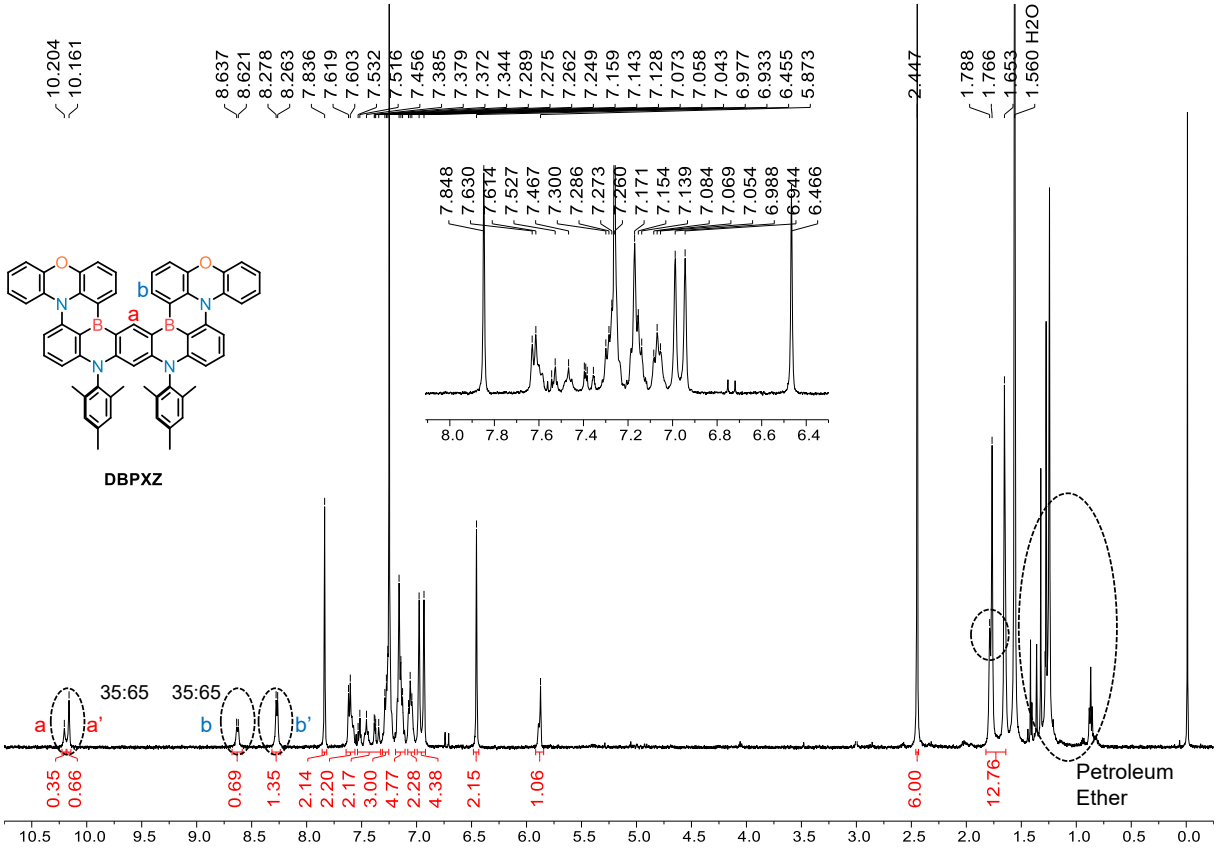

Fig. S1. ^{1}H NMR spectrum of **DBPXZ** in $CDCl_3$ (500 MHz, 25 °C).

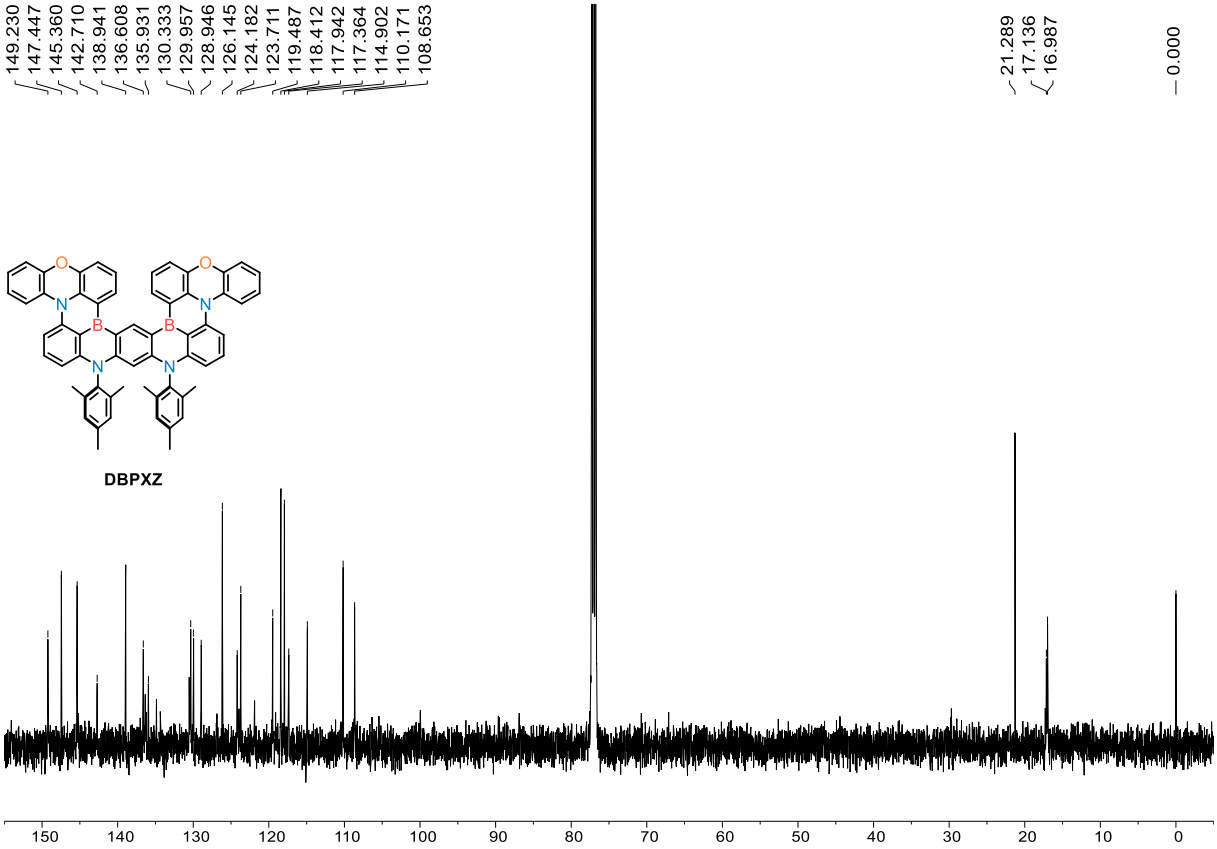

Fig. S2. ^{13}C NMR spectrum of **DBPXZ** in $CDCl_3$ (126 MHz, 25 °C).

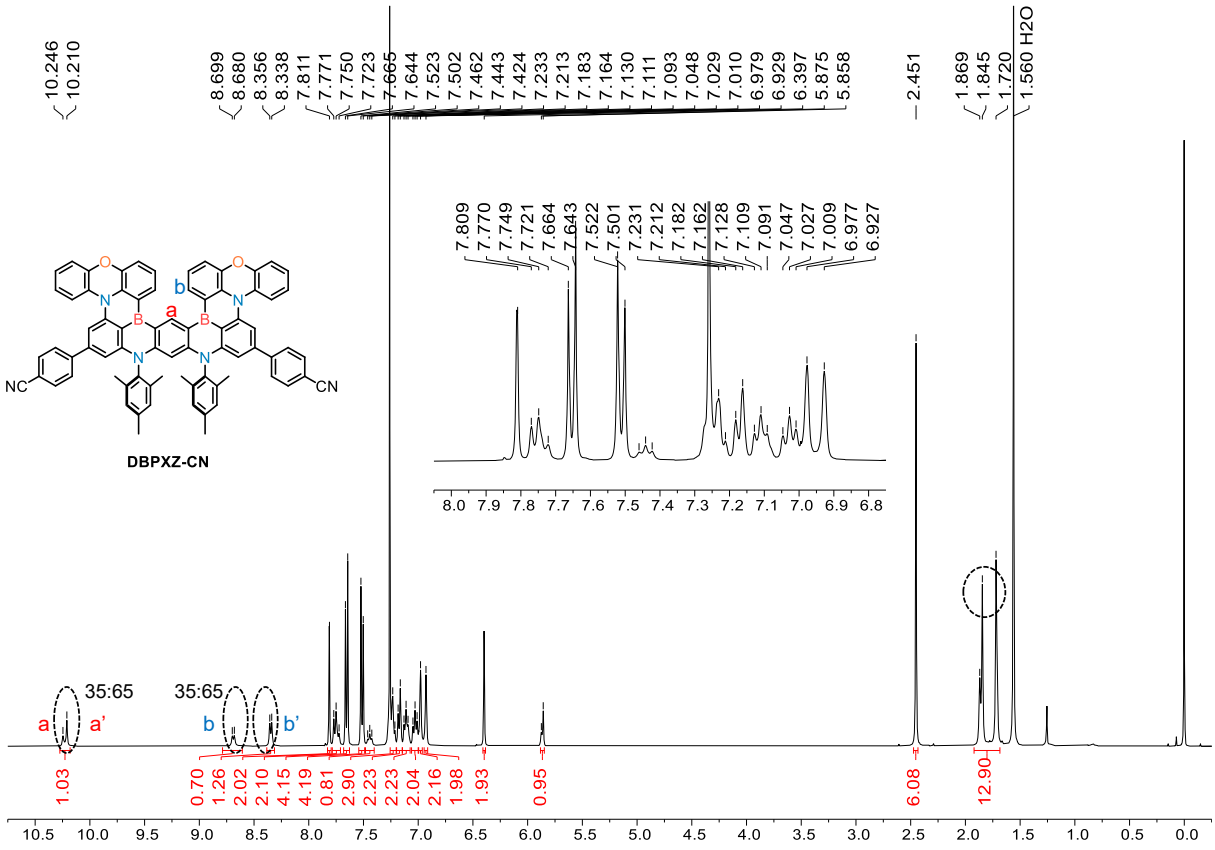

Fig. S3. ^{1}H NMR spectrum of **DBPXZ-CN** in $CDCl_3$ (400 MHz, 25 °C).

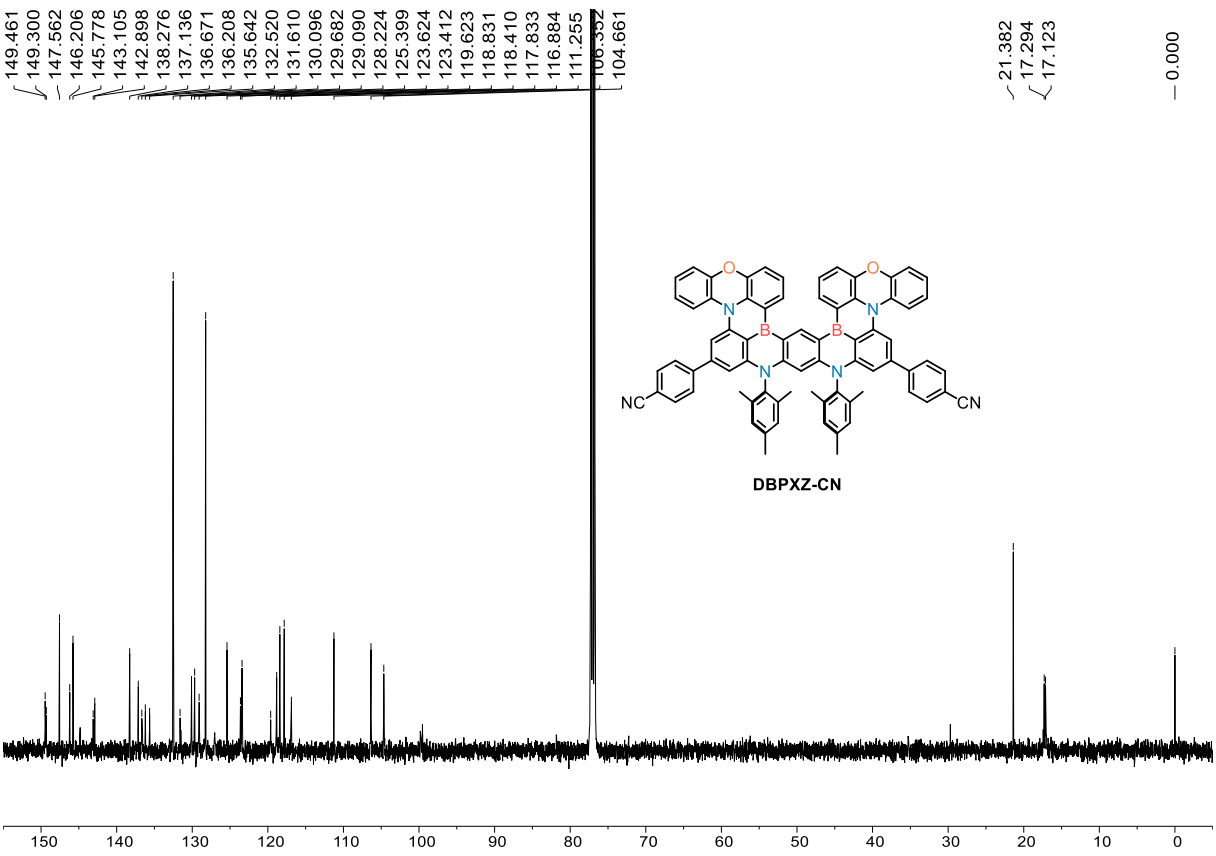

Fig. S4. ^{1}H NMR spectrum of **DBPXZ-CN** in $CDCl_3$ (126 MHz, 25 °C).

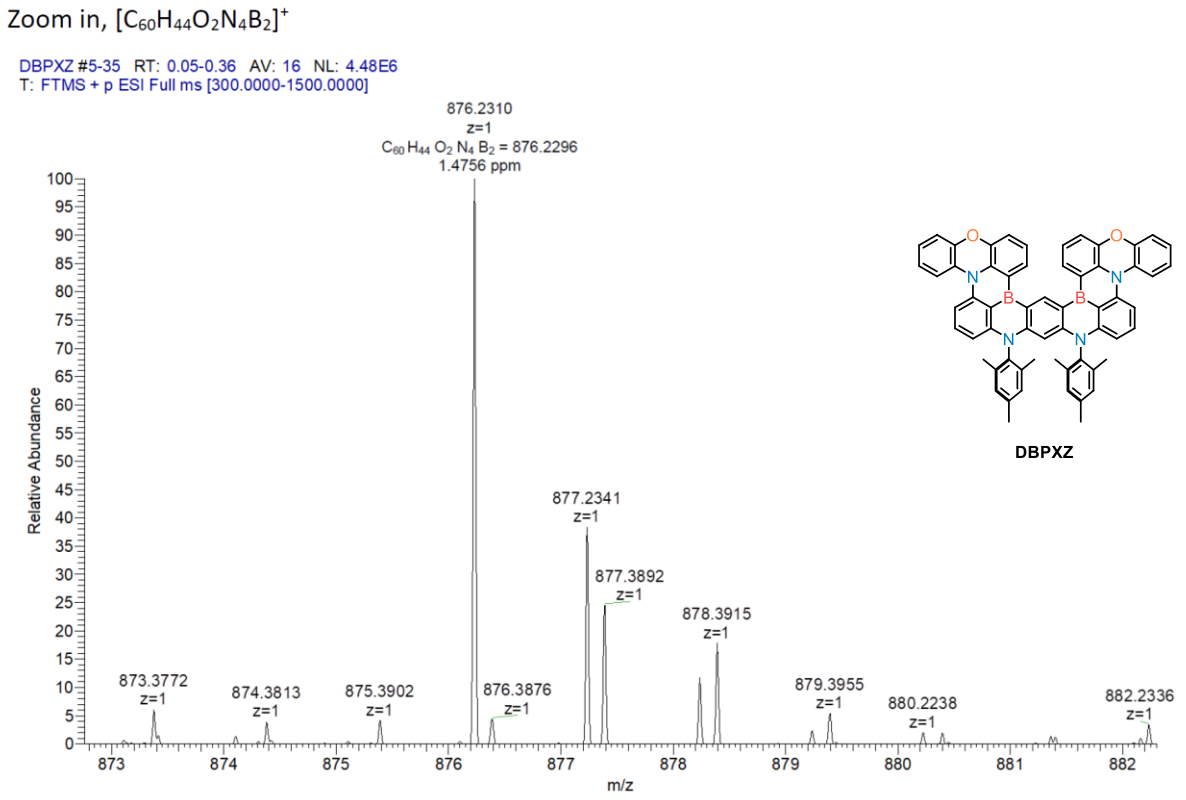

Fig. S5. HR-MS spectrum of **DBPXZ**.

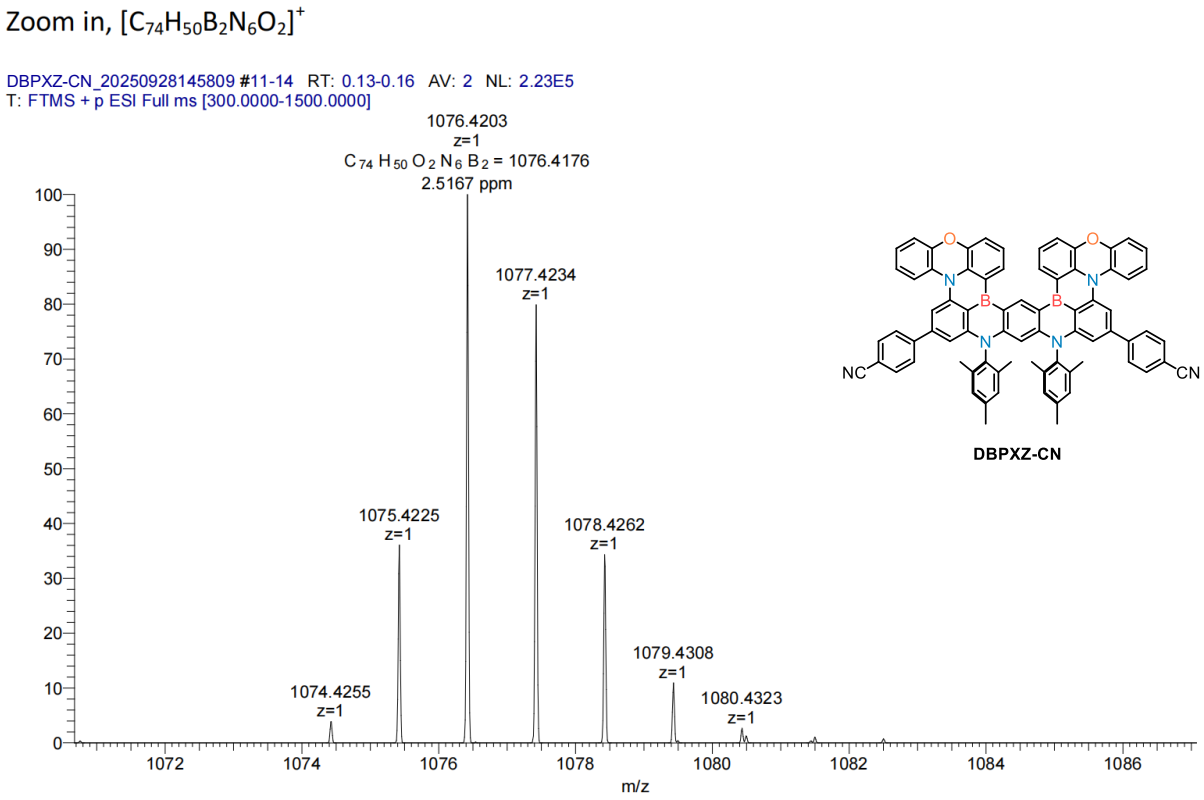

Fig. S6. HR-MS spectrum of **DBPXZ-CN**.

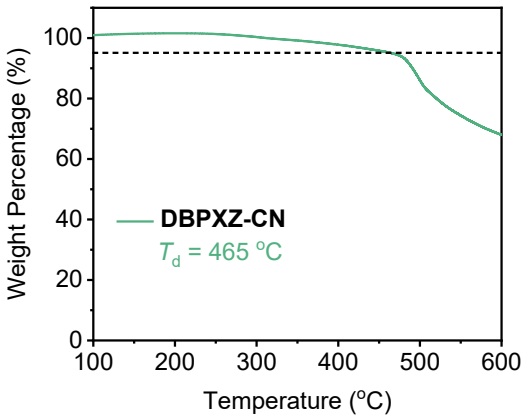

Fig. S7. Thermal gravimetric analysis (TGA) curves at a heating rate of 10 °C min^{-1}.

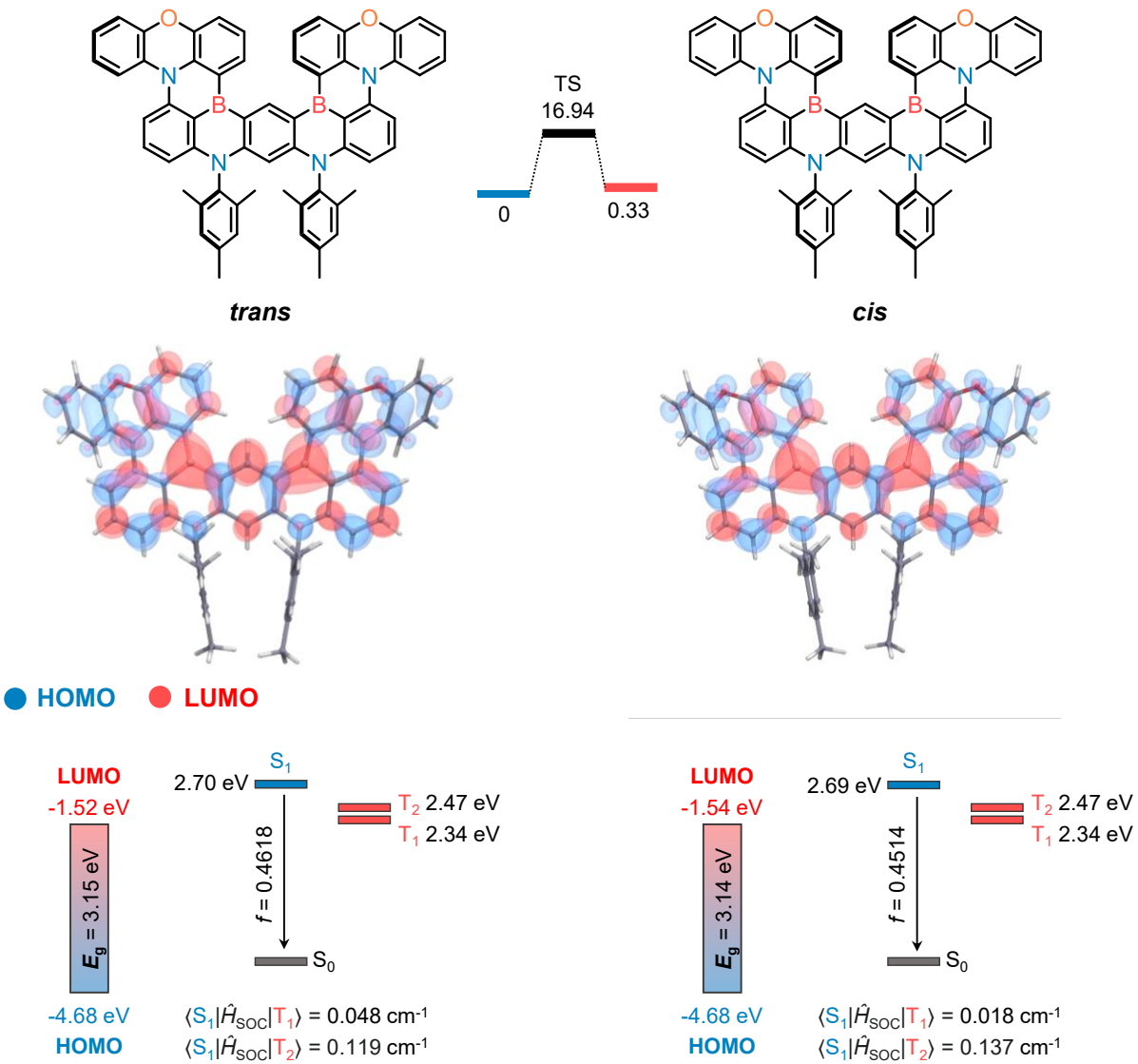

Fig. S8. The Relative Gibbs free energy diagram (in kcal mol^{-1}), molecular structure and frontier molecular orbital distributions (FMOs) and related energy levels of **DBPXZ** at different conformations, *trans* (left) and *cis* (right).

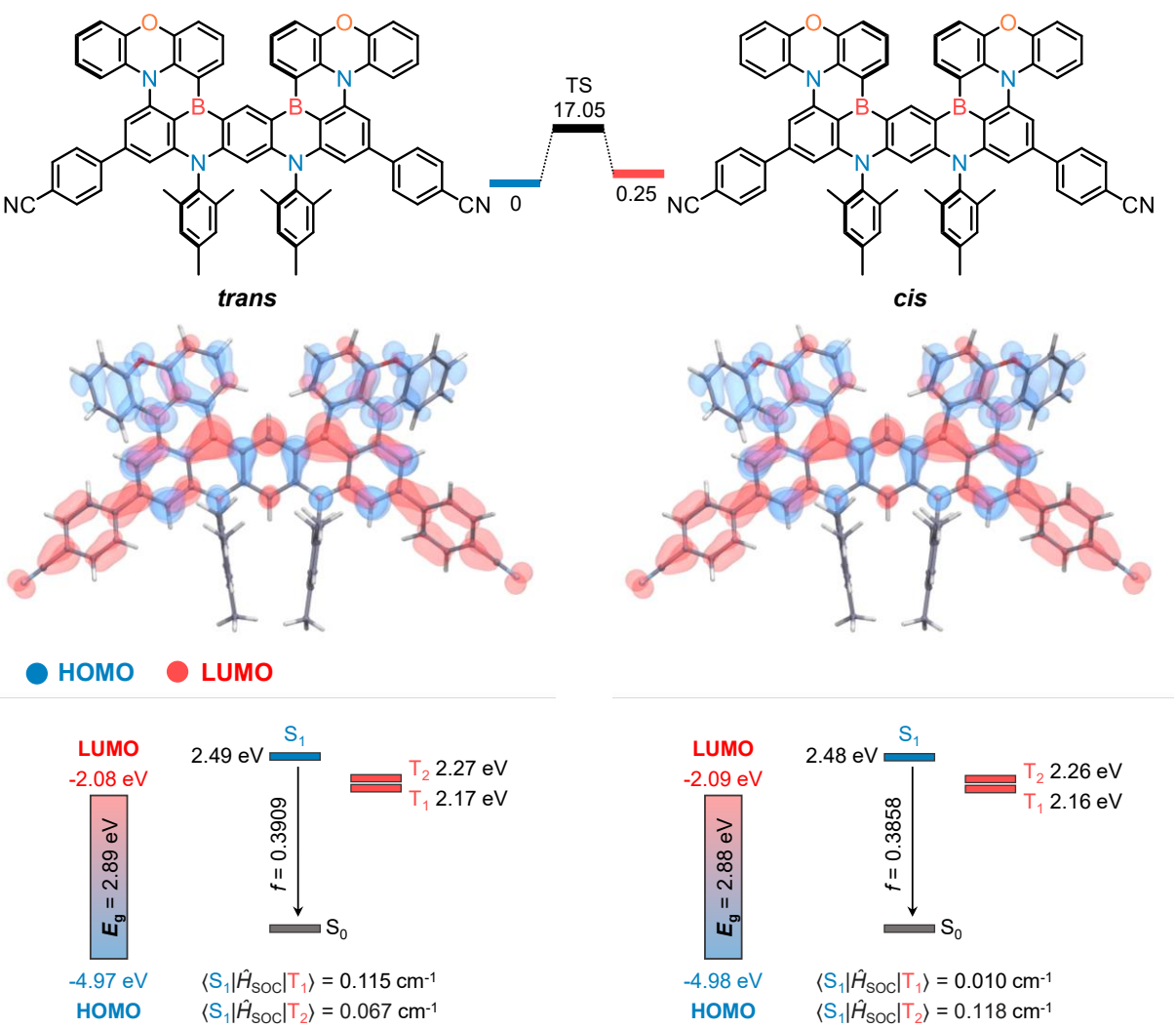

Fig. S9. The Relative Gibbs free energy diagram (in kcal mol^{-1}), molecular structure and frontier molecular orbital distributions (FMOs) and related energy levels of **DBPXZ-CN** at different conformations, *trans* (left) and *cis* (right).

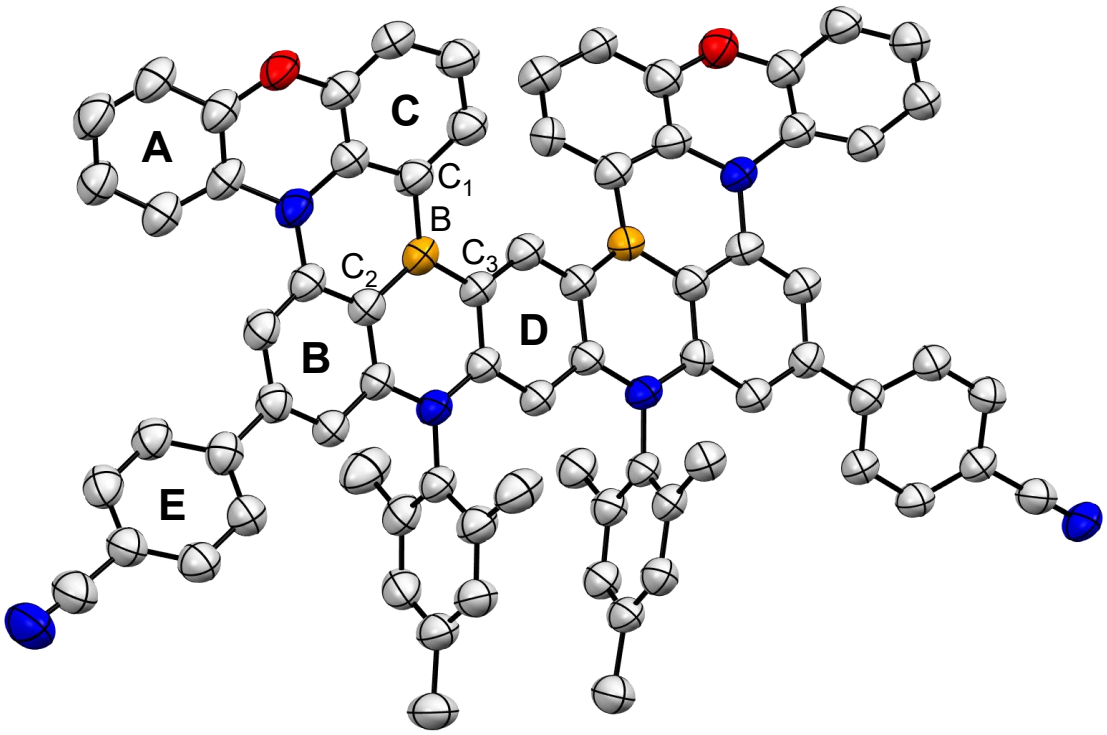

θ_{AB} = 43.09° ∠C_1-B-C_3= 115.45°
θ_{CD} = 26.64° ∠C_1-B-C_3= 128.27°
θ_{BE} = 39.90° ∠C_2-B-C_3= 116.02°

Fig. S10. Single-crystal X-ray diffraction structures of **DBPXZ-CN** (CCDC 2528545).

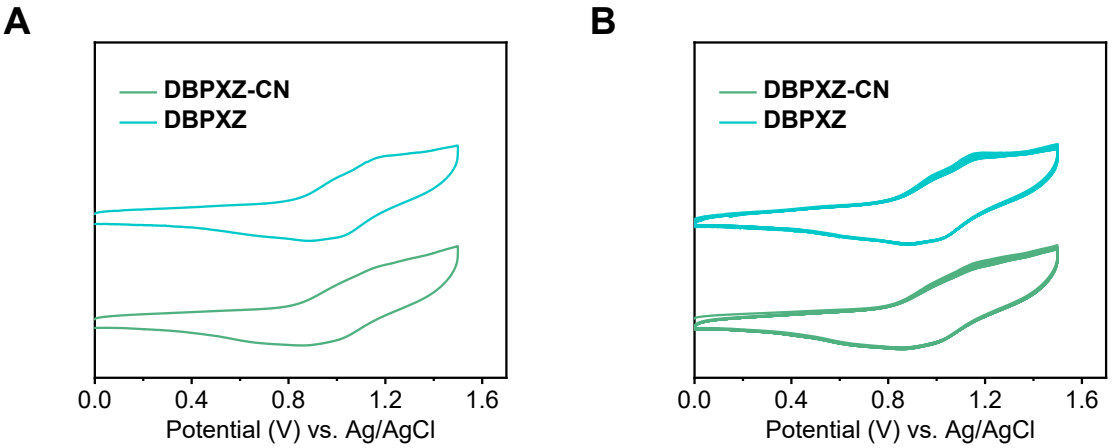

Fig. S11. (A) Oxidation curves of **DBPXZ** and **DBPXZ-CN** measured by cyclic voltammetry (CV). (B) Consecutive oxidation curves over 20 CV cycles. Both compounds exhibit two oxidation waves, which are attributed to successive oxidation processes of the conjugated electron-rich framework.

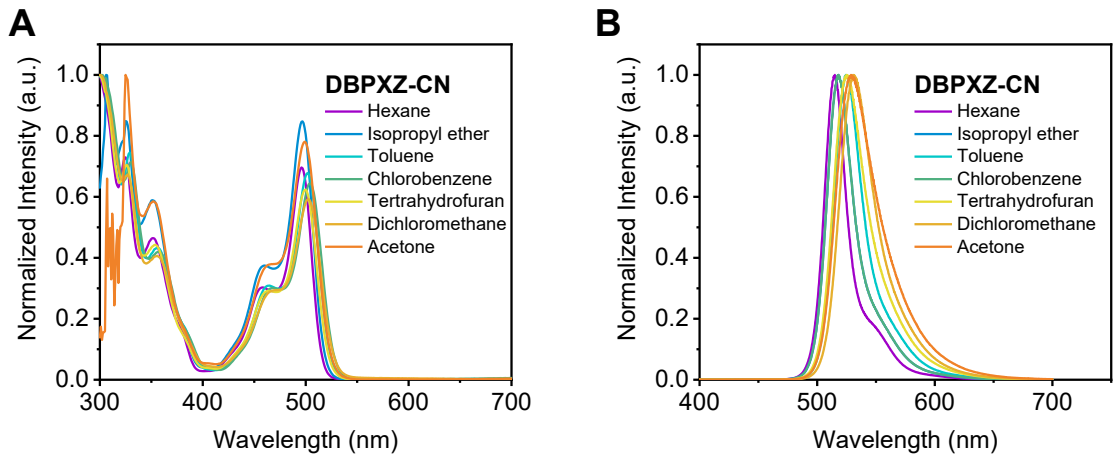

Fig. S12. Absorption and fluorescence spectra of **DBPXZ-CN** recorded in various solvents at a fixed concentration of 1×10^{-5} M.

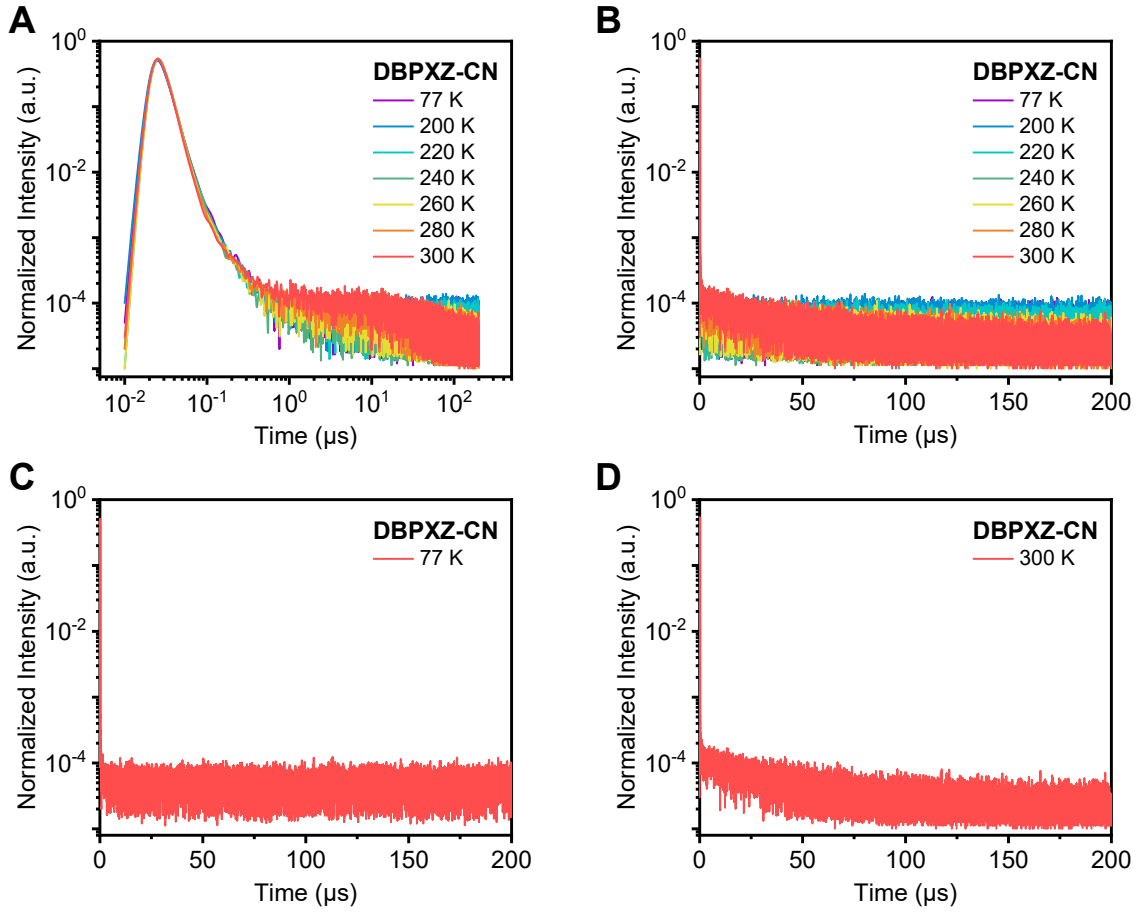

Fig. S13. Temperature-dependent transient photoluminescence (PL) decay characteristics of **DBPXZ-CN**–doped films (2 wt%) in a DMIC-TRZ host. (A) PL decay profiles displayed on double-logarithmic coordinates. (B) PL decay profiles displayed on semi-logarithmic (log–linear) coordinates. (C) Transient PL decay recorded at 77 K. (D) Transient PL decay recorded at 300 K.

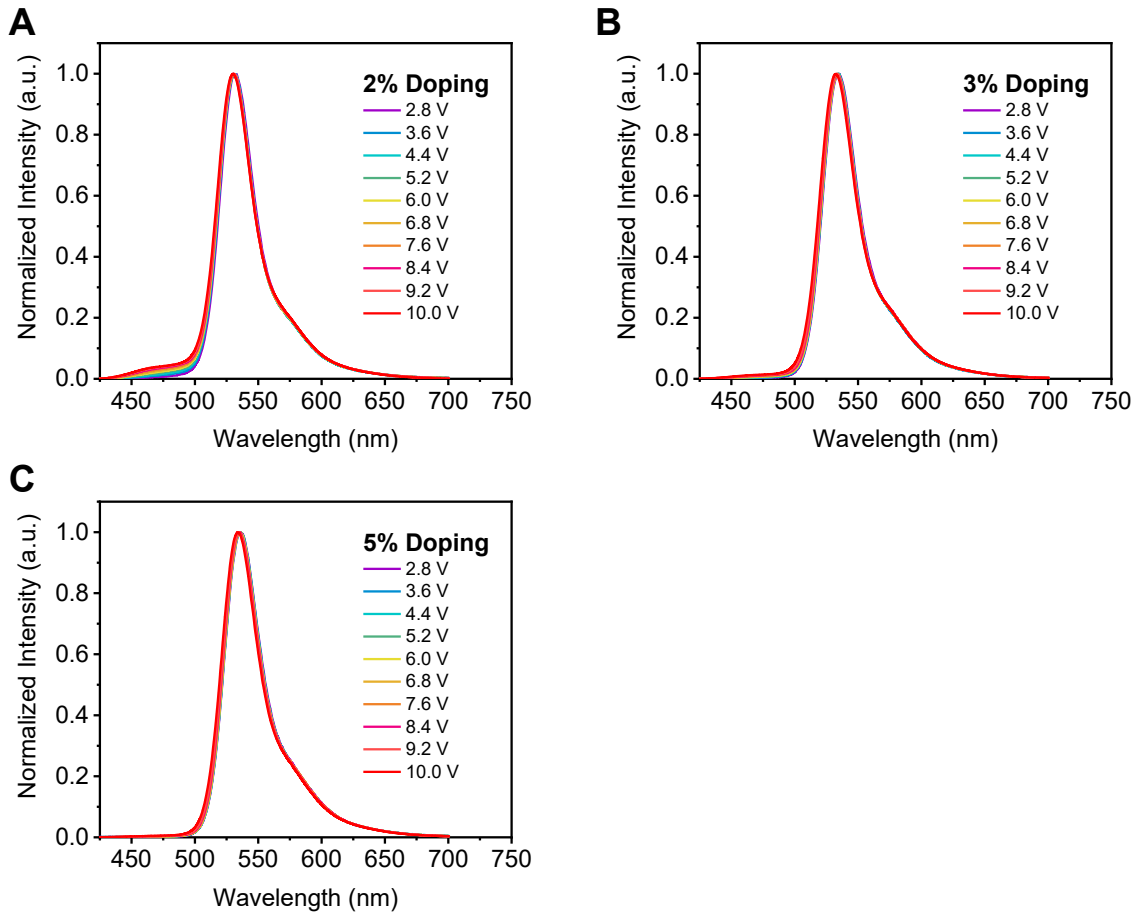

Fig. S14. EL spectra of the devices based on **DBPXZ-CN** at different voltages.

Table S1. Summary of TD-DFT data for **DBPXZ** (*trans*), **DBPXZ** (*cis*), **DBPXZ-CN** (*trans*), and **DBPXZ-CN** (*cis*) calculated at the b3lyp/6-31g(d,p) level.

Compound	Transition	Wavelength (nm)	Energy (eV)	Oscillator Strength	Coefficient of Orbital
DBPXZ (*trans*)	S_0-S_1	458.95	2.70	0.4618	HOMO-1→LUMO+1 (0.0256) HOMO→LUMO (0.9617)
	S_0-T_1	527.01	2.35	0.0000	HOMO-1→LUMO+1 (0.0997) HOMO→LUMO (0.8724)
	S_0-T_2	501.60	2.47	0.0000	HOMO-1→LUMO (0.7178) HOMO→LUMO+1 (0.2388)
DBPXZ (*cis*)	S_0-S_1	461.01	2.69	0.4514	HOMO-1→LUMO+1 (0.0251) HOMO→LUMO (0.9622)
	S_0-T_1	529.48	2.34	0.0000	HOMO-1→LUMO+1 (0.0963) HOMO→LUMO (0.8760)
	S_0-T_2	502.92	2.47	0.0000	HOMO-1→LUMO (0.7225) HOMO→LUMO+1 (0.2341)
DBPXZ-CN (*trans*)	S_0-S_1	498.26	2.49	0.3909	HOMO-1→LUMO+1 (0.1085) HOMO→LUMO (0.8312)
	S_0-T_1	572.55	2.17	0.0000	HOMO-1→LUMO (0.6563) HOMO→LUMO+1 (0.2657) HOMO→LUMO+3 (0.0285)
	S_0-T_2	547.11	2.27	0.0000	HOMO-1→LUMO+1 (0.0314) HOMO→LUMO (0.9539)
DBPXZ-CN (*cis*)	S_0-S_1	499.45	2.48	0.3858	HOMO-1→LUMO+1 (0.0304) HOMO→LUMO (0.9549)
	S_0-T_1	574.15	2.16	0.0000	HOMO-1→LUMO+1 (0.1056) HOMO→LUMO (0.8348)
	S_0-T_2	547.66	2.26	0.0000	HOMO-1→LUMO (0.6591) HOMO→LUMO+1 (0.2636) HOMO→LUMO+3 (0.0287)

Table S2. Cartesian coordinates of **DBPXZ** (*trans*) at the optimized S_0 geometry.

C	1.232013	-0.368825	-0.183043		C	-7.144384	-2.165181	-1.426141
C	1.207473	1.057107	-0.145258		C	-8.237099	-2.848038	-1.959691
C	0.000033	1.745121	0.000153		C	-8.561235	-4.126183	-1.506782
C	-1.207429	1.057108	0.145431		C	-7.765983	-4.735818	-0.536947
C	-1.232003	-0.368826	0.183072		B	2.583435	-1.063058	-0.379393
C	-0.000002	-1.01355	-0.000036		B	-2.583448	-1.063029	0.379435
N	-2.37992	1.807809	0.274239		H	0.000041	2.821643	0.00023
N	2.379985	1.807789	-0.274099		H	-0.000006	-2.094916	-0.000129
C	3.660845	1.248285	-0.290055		H	1.904448	6.086813	1.342385
C	2.237855	3.232405	-0.443961		H	1.754946	5.506595	-2.904487
C	-3.6608	1.248344	0.290111		H	-1.755191	5.50678	2.904464
C	-2.237768	3.232433	0.444028		H	-1.903992	6.086704	-1.342471
C	2.177023	4.063724	0.680663		H	7.237772	-0.289412	-0.335424
C	1.959545	5.430409	0.477993		H	6.926114	2.15036	-0.397304
C	1.801306	5.96594	-0.8021		H	4.677038	3.15918	-0.343634
C	1.874221	5.103934	-1.901712		H	-4.676924	3.159277	0.343513
C	2.088257	3.734267	-1.745211		H	-6.926044	2.150525	0.397018
C	-2.088366	3.734383	1.745256		H	-7.237767	-0.289232	0.335182
C	-1.87431	5.10406	1.901694		H	0.927424	-3.138029	-1.424968
C	-1.801178	5.965982	0.802034		H	1.575957	-5.439715	-2.016085
C	-1.959247	5.430362	-0.478046		H	3.96453	-6.165434	-1.734152
C	-2.17676	4.063678	-0.68065		H	7.960242	-5.742728	0.184277
C	3.805591	-0.16448	-0.280436		H	9.414102	-4.656622	1.916833
C	5.114742	-0.7088	-0.246971		H	8.828603	-2.376439	2.737241
C	6.239973	0.126857	-0.298805		H	6.888341	-1.179341	1.791472
C	6.054497	1.504778	-0.342495		H	-3.96485	-6.165292	1.734394
C	4.788255	2.083129	-0.32428		H	-1.576256	-5.439673	2.016394
C	-4.788179	2.08323	0.324199		H	-0.927588	-3.138063	1.425221
C	-6.054441	1.504916	0.34231		H	-6.888169	-1.179328	-1.791765
C	-6.239953	0.127003	0.298632		H	-8.828409	-2.376423	-2.737592
C	-5.114745	-0.708701	0.246908		H	-9.414093	-4.656495	-1.917015
C	-3.805578	-0.164418	0.280482		H	-7.960431	-5.742518	-0.184245
N	5.257047	-2.104453	-0.195444		C	-2.302047	3.48346	-2.064389
N	-5.257086	-2.104342	0.195379		H	-3.223144	2.901913	-2.168626
C	4.222668	-2.961929	-0.625543		H	-2.301426	4.272331	-2.819915
C	4.581241	-4.273355	-0.984603		H	-1.467491	2.80611	-2.275755
O	5.900618	-4.689025	-0.929421		C	2.139257	2.802914	-2.927445
C	6.684522	-4.046887	0.002851		H	2.012973	3.352144	-3.863118
C	6.379976	-2.738584	0.404374		H	3.093063	2.267039	-2.966686
C	-6.380003	-2.738469	-0.404479		H	1.350982	2.045372	-2.862886

C	-6.684639	-4.046722	-0.002868		C	-2.139573	2.803116	2.927549
O	-5.900833	-4.688804	0.929523		H	-2.013119	3.352368	3.863186
C	-4.581425	-4.273226	0.984697		H	-3.093527	2.267502	2.966849
C	-4.22276	-2.961847	0.625558		H	-1.351508	2.045356	2.86301
C	2.880781	-2.536206	-0.738759		C	2.302474	3.483588	2.064421
C	1.948379	-3.460668	-1.261739		H	3.223658	2.90217	2.168636
C	2.311492	-4.751335	-1.612875		H	2.301789	4.272495	2.819909
C	3.63993	-5.167794	-1.459653		H	1.468025	2.806131	2.275862
C	7.765875	-4.735987	0.536905		C	-1.5341	7.436064	1.005593
C	8.561239	-4.126304	1.506619		H	-2.149637	7.845314	1.812813
C	8.237203	-2.848101	1.959436		H	-0.486302	7.608471	1.276714
C	7.144476	-2.16524	1.425915		H	-1.738855	8.010376	0.098363
C	-3.640185	-5.167691	1.459834		C	1.534314	7.436026	-1.005723
C	-2.311737	-4.751284	1.613099		H	0.486486	7.608514	-1.276654
C	-1.948542	-3.460653	1.261914		H	1.739304	8.010384	-0.098579
C	-2.88086	-2.536175	0.738806		H	2.149744	7.845157	-1.813084

Table S3. Cartesian coordinates of **DBPXZ** (*cis*) at the optimized S_0 geometry.

C	-1.234585	-0.380628	-0.325144	C	6.962245	-2.228778	1.853651
C	-1.22801	1.044269	-0.247916	C	7.994024	-2.949364	2.454589
C	-0.0239	1.751224	-0.196288	C	8.394768	-4.17842	1.932381
C	1.20401	1.084227	-0.206832	C	7.735352	-4.703021	0.821296
C	1.257312	-0.336207	-0.327481	B	-2.591094	-1.094084	-0.350496
C	0.022962	-1.002959	-0.350018	B	2.635669	-1.001562	-0.394146
N	2.368061	1.848815	-0.075823	H	-0.043744	2.824603	-0.117436
N	-2.418667	1.77667	-0.208339	H	0.044139	-2.084938	-0.344655
C	-3.68201	1.19559	-0.068844	H	-2.165364	5.571423	-2.762997
C	-2.320636	3.208659	-0.344067	H	-1.850799	6.012209	1.491503
C	3.651413	1.301238	0.02368	H	1.830536	6.152237	-1.592982
C	2.20402	3.266231	0.133487	H	1.695344	5.48309	2.641087
C	-2.327414	3.755146	-1.635749	H	-7.208894	-0.404447	0.333607
C	-2.162905	5.134109	-1.767662	H	-6.946131	2.041523	0.274926
C	-1.987169	5.962433	-0.653877	H	-4.726381	3.088753	0.045683
C	-1.988724	5.382573	0.616573	H	4.630607	3.215537	0.27973
C	-2.15304	4.005155	0.794975	H	6.885975	2.232426	0.420854
C	2.128014	4.118711	-0.972797	H	7.234113	-0.199955	0.297918
C	1.895999	5.479136	-0.742274	H	-1.073074	-3.111327	-1.673807
C	1.739228	5.98723	0.548501	H	-1.763279	-5.409048	-2.234098
C	1.820121	5.102799	1.630222	H	-4.077995	-6.185098	-1.640427
C	2.04832	3.73946	1.446016	H	-7.776436	-5.876571	0.824196
C	-3.802323	-0.219396	-0.068265	H	-8.996863	-4.852622	2.76242
C	-5.087219	-0.786939	0.128184	H	-8.338596	-2.580294	3.548572
C	-6.221823	0.029117	0.244401	H	-6.561381	-1.330165	2.377124
C	-6.065185	1.41062	0.201498	H	4.266517	-5.947014	-2.022862
C	-4.817005	2.010777	0.061058	H	1.91878	-5.213506	-2.533551
C	4.757903	2.143207	0.21449	H	1.162801	-2.977862	-1.817021
C	6.02691	1.578073	0.305463	H	6.644876	-1.282463	2.271902
C	6.231951	0.203703	0.244757	H	8.476937	-2.546396	3.33867
C	5.125277	-0.641077	0.075312	H	9.200778	-4.737626	2.395536
C	3.820891	-0.104705	-0.076975	H	7.989844	-5.672065	0.406778
N	-5.200905	-2.185536	0.168334	C	2.254347	3.565744	-2.367405
N	5.285935	-2.034753	0.023636	H	3.175386	2.986185	-2.482057
C	-4.223982	-3.014853	-0.420527	H	1.420617	2.891383	-2.592026
C	-4.610441	-4.323449	-0.761048	H	2.253842	4.36855	-3.108135
O	-5.902858	-4.763978	-0.533839	C	2.106751	2.786881	2.610821
C	-6.561195	-4.155592	0.511442	H	3.081529	2.291571	2.666531
C	-6.223388	-2.851249	0.898836	H	1.932056	3.311775	3.552651
C	6.339353	-2.712028	0.698147	H	1.353402	1.998797	2.509632

C	6.71473	-3.976122	0.221832		C	1.479743	7.453454	0.78659
O	6.062214	-4.53716	-0.8533		H	2.214594	7.879934	1.477665
C	4.75205	-4.128427	-1.032996		H	1.522147	8.024345	-0.144288
C	4.327957	-2.858602	-0.60295		H	0.490144	7.61007	1.2294
C	-2.916912	-2.562694	-0.70613		C	-2.117058	3.379293	2.163974
C	-2.055595	-3.457177	-1.379856		H	-2.010028	4.141767	2.938769
C	-2.445053	-4.744479	-1.713394		H	-3.029365	2.807904	2.361998
C	-3.732521	-5.188897	-1.387149		H	-1.276269	2.682927	2.249728
C	-7.550186	-4.874371	1.170683		C	-2.488793	2.860556	-2.836306
C	-8.215208	-4.299075	2.253028		H	-3.419852	2.287689	-2.779463
C	-7.851233	-3.025204	2.687339		H	-2.497731	3.443899	-3.759742
C	-6.850674	-2.312532	2.027066		H	-1.670903	2.134518	-2.895067
C	3.892557	-4.981537	-1.700475		C	-1.783586	7.445477	-0.83586
C	2.585802	-4.561218	-1.979248		H	-1.853324	7.979616	0.115114
C	2.159369	-3.311971	-1.557598		H	-0.796226	7.654971	-1.262447
C	3.002183	-2.434828	-0.839367		H	-2.527752	7.868897	-1.518024

Table S4. Cartesian coordinates of **DBPXZ-CN** (*trans*) at the optimized S_0 geometry.

C	1.237012	1.083263	0.144509		H	-1.896743	-5.347767	1.480021
C	1.210713	-0.342894	0.108454		H	7.238593	0.98932	0.090677
C	-0.00005	-1.031222	-0.000027		H	4.665831	-2.445772	0.232842
C	-1.210797	-0.342871	-0.108559		H	-4.665776	-2.445935	-0.232879
C	-1.237139	1.083279	-0.144634		H	-7.238731	0.98899	-0.090726
C	-0.000059	1.728058	-0.000063		H	0.97864	3.867831	1.374758
N	-2.385892	-1.095247	-0.199789		H	1.658198	6.165856	1.943294
N	2.385857	-1.095228	0.199713		H	4.043865	6.87332	1.6025
C	3.664837	-0.535858	0.176667		H	7.9968	6.418581	-0.399408
C	2.252031	-2.523416	0.348969		H	9.402586	5.322284	-2.164157
C	-3.6649	-0.535958	-0.176725		H	8.776149	3.051557	-2.980061
C	-2.251899	-2.523422	-0.348964		H	6.844	1.87203	-1.998934
C	2.170308	-3.334321	-0.788869		H	-4.044379	6.873233	-1.602468
C	1.97019	-4.706608	-0.605592		H	-1.65868	6.165898	-1.943378
C	1.851521	-5.266694	0.668128		H	-0.979001	3.86791	-1.374936
C	1.943344	-4.423453	1.781292		H	-6.844178	1.871824	1.999037
C	2.140267	-3.049392	1.644658		H	-8.776318	3.051273	2.980198
C	-2.140451	-3.049508	-1.644635		H	-9.402877	5.321975	2.164295
C	-1.943226	-4.423534	-1.781186		H	-7.997166	6.418304	0.399499
C	-1.850765	-5.26662	-0.66796		C	7.256447	-1.703596	0.19554
C	-1.969127	-4.706425	0.605742		C	8.418722	-1.33209	0.89201
C	-2.169538	-3.33417	0.788933		C	7.244691	-2.941262	-0.469808
C	3.80997	0.875596	0.165614		C	9.531436	-2.161732	0.92487
C	5.120628	1.411397	0.09531		H	8.438009	-0.393048	1.434047
C	6.241717	0.572362	0.115448		C	8.350306	-3.780235	-0.444117
C	6.071436	-0.81516	0.162276		H	6.364866	-3.235129	-1.031586
C	4.7877	-1.372968	0.177972		C	9.505451	-3.395465	0.25515
C	-4.787709	-1.373138	-0.178013		H	10.420091	-1.868872	1.472797
C	-6.071472	-0.815402	-0.162318		H	8.333415	-4.729443	-0.968027
C	-6.241826	0.572109	-0.115485		C	-7.256436	-1.703898	-0.195585
C	-5.12079	1.411222	-0.095339		C	-8.418727	-1.332454	-0.892063
C	-3.8101	0.875492	-0.165683		C	-7.244618	-2.941561	0.469767
N	5.268937	2.803948	0.032232		C	-9.531398	-2.162154	-0.924926
N	-5.269185	2.803766	-0.032241		H	-8.438059	-0.393413	-1.434101
C	4.250812	3.668101	0.488939		C	-8.35019	-3.780592	0.444073
C	4.628327	4.976751	0.8386		H	-6.364781	-3.23538	1.031549
O	5.948579	5.382601	0.753099		C	-9.505352	-3.395884	-0.255202
C	6.708187	4.734733	-0.194842		H	-10.420066	-1.869341	-1.472858
C	6.383774	3.430564	-0.592656		H	-8.333253	-4.729797	0.967985
C	-6.384032	3.43034	0.5927		C	10.648662	-4.256463	0.285168

C	-6.70851	4.7345	0.194907		N	11.577051	-4.957201	0.308815
O	-5.94896	5.382419	-0.753036		C	-10.648518	-4.256942	-0.285224
C	-4.628699	4.976619	-0.838586		N	-11.576871	-4.957728	-0.308873
C	-4.251113	3.667978	-0.488958		C	-1.616626	-6.744567	-0.853598
C	2.909432	3.250884	0.639408		H	-0.61753	-6.934338	-1.261047
C	1.997067	4.182946	1.183668		H	-1.697832	-7.285366	0.092501
C	2.37823	5.471597	1.522733		H	-2.339019	-7.176796	-1.553631
C	3.705348	5.878108	1.336352		C	1.617812	-6.744703	0.853843
C	7.78501	5.414635	-0.749808		H	0.618547	-6.93481	1.260722
C	8.553293	4.79946	-1.737468		H	1.69979	-7.28561	-0.092125
C	8.206665	3.52626	-2.188075		H	2.339962	-7.176556	1.55436
C	7.118637	2.853018	-1.633461		C	2.214923	-2.13919	2.842016
C	-3.70579	5.878036	-1.336354		H	2.114171	-2.705892	3.770175
C	-2.378662	5.471599	-1.522799		H	3.167123	-1.599565	2.868938
C	-1.997428	4.18296	-1.183776		H	1.421831	-1.384623	2.810554
C	-2.909715	3.250833	-0.639487		C	-2.257102	-2.728282	2.164694
C	-7.118851	2.852789	1.63354		H	-3.174707	-2.143594	2.283477
C	-8.206884	3.525997	2.188187		H	-2.236897	-3.50279	2.934548
C	-8.55358	4.799177	1.737583		H	-1.417423	-2.047485	2.341748
C	-7.785343	5.414366	0.749901		C	-2.215749	-2.139457	-2.842067
B	2.594135	1.778135	0.296703		H	-2.115251	-2.706246	-3.7702
B	-2.594308	1.778094	-0.296807		H	-3.168058	-1.600011	-2.868681
H	-0.000082	-2.107906	0.000019		H	-1.422783	-1.384741	-2.810998
H	-0.000031	2.80934	-0.000046		C	2.258346	-2.728602	-2.164676
H	1.898291	-5.348061	-1.479829		H	3.175875	-2.143728	-2.283131
H	1.854241	-4.845384	2.7792		H	2.238658	-3.503223	-2.93443
H	-1.854361	-4.84555	-2.77908		H	1.418596	-2.048017	-2.342205

Table S5. Cartesian coordinates of **DBPXZ-CN** (*cis*) at the optimized S_0 geometry.

C	1.253867	1.077566	-0.417587		H	-1.790692	-5.343674	1.257608
C	1.215621	-0.347448	-0.358174		H	7.22663	0.96337	0.19739
C	-0.004406	-1.027817	-0.365441		H	4.650568	-2.46403	-0.026503
C	-1.215752	-0.332349	-0.378193		H	-4.674199	-2.424632	-0.166703
C	-1.238253	1.094534	-0.39733		H	-7.198207	1.013242	0.330892
C	0.01232	1.731228	-0.404775		H	1.130049	3.79942	-1.76652
N	-2.397341	-1.080318	-0.355618		H	1.872351	6.06928	-2.381401
N	2.387547	-1.10644	-0.268725		H	4.223084	6.784586	-1.862284
C	3.663828	-0.550015	-0.1539		H	7.981094	6.406931	0.501638
C	2.241829	-2.533008	-0.110537		H	9.217021	5.386769	2.43138
C	-3.663679	-0.518809	-0.183554		H	8.503308	3.158028	3.290091
C	-2.285396	-2.508551	-0.521819		H	6.656529	1.942132	2.195662
C	2.164844	-3.345048	-1.24673		H	-4.179384	6.906472	-1.458717
C	1.958654	-4.716759	-1.063091		H	-1.852612	6.19681	-2.084072
C	1.829926	-5.2748	0.210122		H	-1.120825	3.890578	-1.619586
C	1.912106	-4.429377	1.322787		H	-6.56646	1.862563	2.378006
C	2.113778	-3.056298	1.185989		H	-8.371884	3.031271	3.587712
C	-2.29713	-3.029794	-1.823776		H	-9.078365	5.314708	2.880125
C	-2.12597	-4.405134	-1.982548		H	-7.877479	6.433812	0.983404
C	-1.939966	-5.25374	-0.885653		C	7.230396	-1.73234	0.223439
C	-1.936927	-4.698108	0.395762		C	8.458292	-1.399584	-0.37269
C	-2.107539	-3.325305	0.601294		C	7.142038	-2.93745	0.940901
C	3.819037	0.859191	-0.19448		C	9.560981	-2.235403	-0.258471
C	5.121975	1.3931	-0.026313		H	8.539141	-0.487099	-0.953042
C	6.233092	0.549754	0.097985		C	8.236872	-3.782179	1.061857
C	6.056001	-0.837659	0.101285		H	6.208772	-3.200397	1.426736
C	4.774961	-1.390378	-0.009627		C	9.458188	-3.43626	0.461723
C	-4.783851	-1.352912	-0.076915		H	10.501481	-1.972997	-0.729954
C	-6.055024	-0.792625	0.094146		H	8.160099	-4.705786	1.624723
C	-6.212493	0.594126	0.186291		C	-7.240101	-1.677608	0.178368
C	-5.092574	1.429771	0.094528		C	-8.472673	-1.289648	-0.373201
C	-3.799997	0.89248	-0.13094		C	-7.157959	-2.928458	0.813435
N	5.274565	2.786526	-0.007824		C	-9.585586	-2.115988	-0.294916
N	-5.227396	2.821371	0.196463		H	-8.549642	-0.339877	-0.890867
C	4.307035	3.634229	-0.587694		C	-8.263011	-3.7643	0.897795
C	4.723893	4.923726	-0.962723		H	-6.221008	-3.235569	1.264924
O	6.0346	5.327539	-0.779924		C	-9.488789	-3.36296	0.343035
C	6.703044	4.720014	0.25927		H	-10.52972	-1.8102	-0.731725
C	6.335012	3.436293	0.684785		H	-8.190608	-4.723919	1.397446
C	-6.262638	3.440767	0.951514		C	10.590662	-4.30336	0.583367

C	-6.625717	4.750894	0.610925		N	11.510223	-5.00903	0.683104
O	-5.976653	5.410776	-0.4083		C	-10.631838	-4.220574	0.427226
C	-4.677045	5.002936	-0.651599		N	-11.560013	-4.918582	0.496385
C	-4.265889	3.689498	-0.362645		C	-1.733964	-6.732468	-1.096865
C	2.980638	3.216241	-0.833763		H	-0.759364	-6.929652	-1.556998
C	2.12795	4.124024	-1.500317		H	-1.772324	-7.281729	-0.152828
C	2.546634	5.393465	-1.865552		H	-2.496625	-7.149191	-1.762498
C	3.855043	5.804143	-1.58107		C	1.600054	-6.753209	0.397222
C	7.731704	5.420586	0.876409		H	0.624467	-6.94335	0.857426
C	8.404886	4.848135	1.954927		H	1.629343	-7.287247	-0.555658
C	8.009923	3.5981	2.429977		H	2.358468	-7.193139	1.053473
C	6.97018	2.904215	1.81186		C	2.173981	-2.146794	2.384909
C	-3.81565	5.907659	-1.244555		H	2.020137	-2.708915	3.308623
C	-2.521089	5.499796	-1.589345		H	3.141667	-1.638249	2.447312
C	-2.108109	4.207184	-1.30901		H	1.407784	-1.367023	2.323821
C	-2.952272	3.27119	-0.671026		C	2.266107	-2.740089	-2.621682
C	-6.877403	2.849286	2.060096		H	1.422015	-2.06797	-2.811495
C	-7.893681	3.516336	2.743363		H	3.179042	-2.146068	-2.727276
C	-8.2845	4.79657	2.352858		H	2.26569	-3.515295	-3.391032
C	-7.630675	5.424623	1.29349		C	-2.069065	-2.725632	1.982044
B	2.624962	1.760734	-0.459818		H	-2.982836	-2.161738	2.195176
B	-2.602343	1.794238	-0.382503		H	-1.955761	-3.502102	2.741797
H	-0.012149	-2.103782	-0.330133		H	-1.231296	-2.026973	2.078562
H	0.02172	2.812139	-0.354103		C	-2.473821	-2.113988	-3.006055
H	1.892923	-5.359325	-1.936922		H	-2.479595	-2.679329	-3.940476
H	1.808703	-4.848813	2.320466		H	-3.412084	-1.554419	-2.935261
H	-2.132801	-4.823624	-2.985797		H	-1.665451	-1.37664	-3.054152

Table S6. Crystal data and structure refinement for **DBPXZ-CN**.

Empirical formula	$C_{74}H_{50}B_2N_6O_2$
Formula weight	1076.82
Temperature/K	170.00
Crystal system	triclinic
Space group	P-1
a/Å	12.7168(8)
b/Å	13.4458(8)
c/Å	19.0183(11)
α/°	76.255(4)
β/°	74.047(4)
γ/°	64.632(3)
Volume/Å^3	2798.2(3)
Z	2
ρ_{calc}g/cm^3	1.278
μ/mm^{-1}	0.601
F(000)	1124.0
Crystal size/mm^3	0.1 × 0.05 × 0.05
Radiation	CuKα (λ = 1.54178)
2Θ range for data collection/°	4.88 to 140.54
Index ranges	-15 ≤ h ≤ 15, -15 ≤ k ≤ 16, -23 ≤ l ≤ 23
Reflections collected	51888
Independent reflections	10314 [R_{int} = 0.0672, R_{sigma} = 0.0448]
Data/restraints/parameters	10314/0/764
Goodness-of-fit on F^2	1.054
Final R indexes [I>=2σ (I)]	R_1 = 0.1155, wR_2 = 0.2726
Final R indexes [all data]	R_1 = 0.1746, wR_2 = 0.3240
Largest diff. peak/hole / e Å^{-3}	0.34/-0.33

Table S7. The emission profiles of emitters in solution states.

Solvent	**DBPXZ-CN**	
	λ_{em} (nm)	FWHM (nm, meV)
Hexane	515	22, 104
Isopropyl ether	518	27, 123
Toluene	525	28, 129
Chlorobenzene	518	26, 121
Tetrahydrofuran	526	34, 151
Dichloromethane	532	35, 153
Acetone	530	42, 181

Table S8. The physical data of the emitters.

Emitter	λ_{abs}[a] [nm]	λ_{em}[a/b] [nm]	FWHM[a/b] [nm]	ΔE_{ST}[c] [eV]	Φ_{PL}[d] [%]	τ_{PF}[d] [ns]	τ_{DF}[d] [μs]	k_r[e] [10^7 s^{-1}]	k_{nr}[e] [10^6 s^{-1}]	k_{ISC}[e] [10^7 s^{-1}]	k_{RISC}[e] [10^4 s^{-1}]
DBPXZ	460	485/490	35/54	0.17	-	-	-	-	-	-	-
DBPXZ-CN	502	525/535	28/32	0.13	98	6.2	32.0	7.9	1.6	8.1	6.3

[a] Absorption maximum (λ_{abs}), fluorescence maximum (λ_{em}), and full-width at half-maximum (FWHM) of fluorescence spectrum measured in toluene (1×10^{-5} M). [b] λ_{em} and corresponding FWHM measured in DMIC-TRZ film. [c] Energy gap between S_1 and T_1 estimated from the fluorescence and phosphorescence maxima in toluene at 77 K. [d] Photoluminescence quantum yield (Φ_{PL}), prompt (τ_{PF}) and delayed (τ_{DF}) fluorescence lifetime measured in DMIC-TRZ film. [e] Associated rate constants of radiative decay (k_r), non-radiative decay (k_{nr}), intersystem crossing (k_{ISC}) and reverse intersystem crossing (k_{RISC}).

Table S9. Key device data of binary green OLEDs

Dop. (wt.%)	λ_{EL}[a] (nm)	FWHM[b] (nm)	CIE[c] (x, y)	V_{on}[d] (V)	L_{max}[e] (cd m^{-2})	CE_{max}[f] (cd A^{-1})	PE_{max}[g] (lm W^{-1})	$EQE_{max/1000}$[h] (%)
2%	531	32	(0.28, 0.68)	2.4	67884	138.0	180.6	33.7/21.9
3%	534	33	(0.30, 0.67)	2.4	118162	147.7	193.3	35.4/24.1
5%	536	34	(0.32, 0.66)	2.4	116648	151.0	197.7	36.5/23.7

[a] Electroluminescence peak wavelength; [b] Full-width at half-maximum; [c] Commission Internationale de l'Eclairage coordinates, values taken at 4 V; [d] Turn-on voltage at 1 cd m^{-2}; [e] Maximum luminance; [f] Maximum current efficiency; [g] Maximum power efficiency; [h] External quantum efficiency: maximum and values at 1000 cd m^{-2}.

References

[1] S. Xiao, X. Cao, G. Chen, X. Yin, Z. Chen, J. Miao, C. Yang, *Angew. Chem. Int. Ed.* **2025**, *64*, e202418348.

[2] V. Dolomanov, L. J. Bourhis, R. J. Gildea, J. A. Howard, H. Puschmann, *J. Appl. Cryst.*, **2009**, *42*, 339-341.

[3] G. M. Sheldrick, *Acta Cryst.*, **2015**, *A71*, 3-8.

[4] G. M. Sheldrick, *Acta Cryst.*, **2015**, *C71*, 3-8.

[5] X. Gao, S. Bai, D. Fazzi, T. Niehaus, M. Barbatti, W. Thiel, *J. Chem. Theory Comput.* **2017**, *13*, 515-524.

[6] Q. Zhang, H. Kuwabara, W. J. Potscavage, S. Huang, Y. Hatae, T. Shibata, C. Adachi, *J. Am. Chem. Soc.* **2014**, *136*, 18070-18081.

[7] Q. Zhang, B. Li, S. Huang, H. Nomura, H. Tanaka, C. Adachi, *Nat. Photon.* **2014**, *8*, 326-332.

[8] T.-L. Wu, M.-J. Huang, C.-C. Lin, P.-Y. Huang, T.-Y. Chou, R.-W. Chen-Cheng, H.-W. Lin, R.-S. Liu, C.-H. Cheng, *Nat. Photon.* **2018**, *12*, 235-240.